Ultimate On-Chip Quantum Amplifier

O. V. Astafiev,[1] A. A. Abdumalikov, Jr.,[2,†] A. M. Zagoskin,[3] Yu. A. Pashkin,[1,*] Y. Nakamura,[1] and J. S. Tsai[1]

[1]*NEC Nano Electronics Research Laboratories, Tsukuba, Ibaraki 305-8501, Japan and RIKEN Advanced Science Institute, Tsukuba, Ibaraki 305-8501, Japan*

[2]*RIKEN Advanced Science Institute, Tsukuba, Ibaraki 305-8501, Japan*

[3]*Department of Physics, Loughborough University, Loughborough, LE11 3TU Leicestershire, United Kingdom*

(Received 14 January 2010; published 6 May 2010)

We report amplification of electromagnetic waves by a single artificial atom in open 1D space. Our three-level artificial atom—a superconducting quantum circuit—coupled to a transmission line presents an analog of a natural atom in open space. The system is the most fundamental quantum amplifier whose gain is limited by a spontaneous emission mechanism. The noise performance is determined by the quantum noise revealed in the spectrum of spontaneous emission, also characterized in our experiments.

DOI: 10.1103/PhysRevLett.104.183603 PACS numbers: 42.50.Gy, 42.50.Nn, 74.78.Na, 85.25.Cp

The quantum amplifiers are actively used devices and most of them rely on natural intra-atomic or molecular transitions with almost untunable transition frequencies [1,2]. Demonstration of amplification on a single atom or molecule in open space is possible [3], however, extremely difficult due to another common characteristic of natural atoms (molecules, quantum dots): They are relatively weakly coupled to the spatial electromagnetic waves in real experiments [3–8], in spite of theoretical feasibility of perfect coupling by careful matching of the spacial modes to the atom [9]. An alternative approach is coupling of the atoms to a field of a high quality resonator [10–15], which has been successfully used to demonstrate lasing action on single natural [16,17] and artificial [18,19] atoms. In the resonators, the atom is coupled to a single mode. On the other hand, an elementary (ultimate) quantum amplifier avoids this limitation and can be realized on a single atom strongly coupled to a continuum of electromagnetic modes of open space. The matching problem of spacial modes of electromagnetic waves can be solved by reducing space dimensionality to a 1D [20,21]. Recently, the highly efficient coupling of an artificial atom to an open 1D transmission line has been achieved experimentally [22].

We demonstrate amplification on a single three-level artificial atom coupled to a 1D transmission line. The atom is a fully controllable and tunable quantum system, with all its basic characteristics, such as energy splitting and coupling to the line, designed in accordance with our requirements. Our demonstration opens the perspective of developing a new type of on-chip quantum amplifiers and other quantum devices, capable of both reproducing the known quantum-optical phenomena and realizing the novel ones, which will use the tunability, controllability, and strong coupling.

Our device is a multilevel quantum system based on the "flux qubit" geometry [23] (a superconducting loop with four tunnel junctions), coupled to a 1D transmission line through the loopline mutual inductance M [24]. We limit our consideration to the three lowest energy states of the system $|i\rangle$ $(i = 1, 2, 3)$ with energies $\hbar\omega_i$ schematically shown in Fig. 1(a). The device is designed in such a way that all relevant transition frequencies of the three-level system $\omega_{ij} = \omega_i - \omega_j$ $(i > j)$ fall within the frequency band of our transmission line and within the working range of our microwave sources, limited by 40 GHz. The system is strongly anharmonic, which prevents nonresonant transitions. The energies of the atomic levels are tuned by the external magnetic field. The transition frequencies ω_{21}, ω_{32}, and ω_{31} reach their extremal values, when the induced magnetic flux in the loop Φ equals to half a flux quantum $(\Phi_0/2)$, that is $\delta\Phi = \Phi - \Phi_0/2 = 0$. Our experiment is performed at the temperature $T = 40$ mK, low compared to the atomic energy splitting $(\hbar\omega_{ij} \gg k_B T)$, which guarantees the absence of thermal excitations.

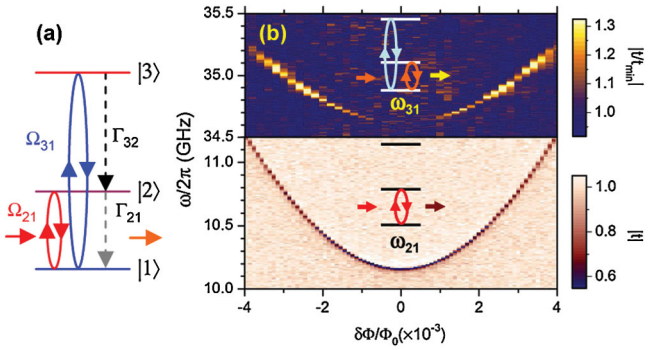

FIG. 1 (color). Spectroscopy of the single artificial three-level atom. (a) Sketch of a three-level artificial atom. Population inversion is created by pumping the atom from the ground state $|1\rangle$ to the second excited state $|3\rangle$ in the relaxation process $|3\rangle \rightarrow |2\rangle$. Ω_{31} and Ω_{21} are the pumping and probing Rabi frequencies, which are used to express the field amplitudes. (b) Spectroscopy of the single three-level atom. The lowest transition frequency ω_{21} is detected by measuring direct transmission. The higher transition frequency ω_{31} is found in the two-wave spectroscopy, and is seen as a bright line.

In the rotating wave approximation, the three-level system is described by the Hamiltonian

$$H_a = -\hbar(\delta\omega_{21}\sigma_{22} + \delta\omega_{31}\sigma_{33}), \quad (1)$$

where $\sigma_{ij} = |i\rangle\langle j|$ is the atomic projection or transition operator, $\delta\omega_{ij} = \omega_{ij}^d - \omega_{ij}$ and $|\delta\omega_{ij}| \ll \omega_{ij}$. The external pumping microwave fields at frequencies ω_{31}^d and ω_{21}^d couple atomic states according to the interaction Hamiltonian

$$H_{\text{int}} = -\hbar\left[\frac{\Omega_{31}}{2}(\sigma_{31} + \sigma_{13}) + \frac{\Omega_{21}}{2}(\sigma_{21} + \sigma_{12})\right], \quad (2)$$

where $\hbar\Omega_{ij} = \phi_{ij}I_{ij}$ is the dipole interaction energy for the transition $|i\rangle \leftrightarrow |j\rangle$ under the influence of the field in the transmission line with the actual current given by $\text{Re}[I_{ij}(0, t)] = I_{ij}\cos\omega_{ij}^d t$. Here we assume that our pointlike atom is situated at $x = 0$ and the waves $I_{ij}(x, t) = I_{ij}\exp(ik_{ij}x - i\omega_{ij}^d t)$ with the wave vector k_{ij} propagate in the transmission line. The dipole matrix element can be presented in the form $\phi_{ij} = \zeta_{ij}MI_p$ with the dimensionality of a magnetic flux, where the dimensionless matrix element satisfies the relation $0 \le \zeta_{ij} \le 1$.

The atomic dynamics is described by the standard master equation $\dot{\rho} = -(i/\hbar)[H, \rho] + L[\rho]$ for the density matrix $\rho = \sum_{i,j}\rho_{ij}|i\rangle\langle j|$ with the Lindblad term $L = \Gamma_{32}\rho_{33}(-\sigma_{33} + \sigma_{22}) + \Gamma_{21}\rho_{22}(-\sigma_{22} + \sigma_{11}) + \sum_{i\neq j}\gamma_{ij}\rho_{ij}\sigma_{ij}$. Here $\gamma_{ij} = \gamma_{ji}$ is the damping rate of the off-diagonal terms (dephasing) and Γ_{ij} is the relaxation rate between the levels $|i\rangle$ and $|j\rangle$ $(i > j)$. In the ladder-type three-level atom $\Gamma_{31} \ll (\Gamma_{32}, \Gamma_{21})$ holds. The low temperature condition suggests suppression of the excitation rates $\Gamma_{12} = 0$, $\Gamma_{23} = 0$, and $\Gamma_{13} = 0$.

The atom in 1D open space generates a scattered wave at frequency ω_{21}^d [22]

$$I_{\text{sc}}(x, t) = i\frac{\hbar\Gamma_{21}}{\phi_{21}}\langle\sigma_{12}\rangle e^{ik_{21}|x| - i\omega_{21}^d t}, \quad (3)$$

where $\langle\sigma_{ij}\rangle = \text{tr}[\sigma_{ij}\rho] = \rho_{ji}$ can be straightforwardly found in the stationary conditions $(\dot{\rho} = 0)$. The transmission coefficient, found as a ratio of the resulting current $I_{21}(x, t) + I_{\text{sc}}(x, t)$ at $x > 0$ to the incident one $I_{21}(x, t)$, takes the form $t = 1 + i(\Gamma_{21}/\Omega_{21})\rho_{21}$, and the amplification condition is $|t| > 1$.

The solution of the master equation [25] is simplified for the most interesting case of nearly resonant drives and fast $|3\rangle \to |2\rangle$ relaxation $(\Gamma_{32} \gg \Gamma_{21})$, when the state $|3\rangle$ remains nearly unpopulated $(\rho_{33} < \Gamma_{21}/\Gamma_{32} \ll 1)$. Neglecting the terms $O(\Gamma_{21}/\Gamma_{32})$, we obtain

$$t \approx 1 + \frac{\Gamma_{21}(\rho_{22} - \rho_{11})}{2\lambda_{21} + \Omega_{31}^2/(2\lambda_{23})}, \quad (4)$$

where $\lambda_{21} = \gamma_{21} - i\delta\omega_{21}$, $\lambda_{23} = \gamma_{32} + i\delta\omega_{31} - i\delta\omega_{21}$. In the resonance, this equation gives the standard population inversion condition for the amplification, $\rho_{22} > \rho_{11}$, with the required pumping amplitude

$$\Omega_{31} > \sqrt{\Gamma_{21}\Gamma_{32}} \quad (5)$$

for weak pure dephasing between the ground and the second excited states $(\gamma_{31} \approx \Gamma_{32}/2)$ [25].

To characterize the energy structure of our atom we perform transmission spectroscopy by sweeping frequency of a weak probe microwave versus the flux bias $\delta\Phi$. The transmitted wave is suppressed due to efficient resonant scattering [22], and reveals the transition frequency ω_{21} as a dark narrow line in $|t|$ on the lower panel of the intensity plot in Fig. 1(b). The higher frequency transition between states $|3\rangle$ and $|1\rangle$ cannot be probed in the direct transmission, since the high frequency cutoff of our cryogenic amplifier (13 GHz) is lower than ω_{31}. To detect ω_{31} we use two-wave spectroscopy in the following way. The probe microwave is adjusted to the minimal transmission $|t_{\text{min}}|$, taking place at $\omega_{21}^d = \omega_{21}$. Simultaneously, we sweep the second high frequency ω_{31}^d. When the transition at ω_{31} occurs, $|t|$ is increased, as the population of the level $|1\rangle$ is reduced and, therefore, we observe a bright line in the intensity plot $|t/t_{\text{min}}|$ versus $\delta\Phi$ [the upper panel of Fig. 1(b)].

At $\delta\Phi = 0$ the system forms the so-called a ladder-type three-level atomic system, in which the selection rule prohibits transitions between levels $|1\rangle$ and $|3\rangle$ due to symmetry of eigenstate wave functions. This is seen as the vanishing spectroscopic line in the upper panel of Fig. 1(b) at $\omega/2\pi = 34.61$ GHz. To achieve population inversion, we must be able to pump the atom from the ground ($|1\rangle$) to the second excited state ($|3\rangle$), therefore, we choose our working point at $\delta\Phi/\Phi_0 = 3.5 \times 10^{-3}$, slightly away from $\delta\Phi = 0$. Driving the system at $\omega_{31}/2\pi = 35.11$ GHz, we expect the cascade relaxation $|3\rangle \to |2\rangle \to |1\rangle$, accompanied by photon emission at frequencies $\omega_{32} = 24.15$ and $\omega_{21} = 10.96$ GHz. The lowest transition can be detected, since it is within our cryogenic amplifier frequency band.

Figure 2(a) shows the measured spontaneous emission spectrum under the resonant pumping at ω_{31} with an amplitude $\Omega_{31}/2\pi = 24$ MHz, which confirms that the mechanism of the level $|2\rangle$ population is implemented. At a weak pumping amplitude $(\Omega_{31}/2 \ll (\gamma_{32}, \gamma_{21}))$, the state $|2\rangle$ population ρ_{22} together with the spontaneous emission rate Γ_{21} define the spectral density of the emission in one of the two possible directions via

$$S(\omega) \approx \frac{\rho_{22}\hbar\omega_{21}\Gamma_{21}}{2\pi}\frac{\gamma_{21}}{\gamma_{21}^2 + (\omega - \omega_{21})^2}. \quad (6)$$

Although in our case $\Omega_{31}/2$ is not negligible comparing γ_{21}, the linewidth $\Delta\omega \approx 2\gamma_{21}$ is still mainly determined by $\gamma_{21}/2\pi \approx 18$ MHz [25]. The intensity plot in Fig. 2(b) shows the spontaneous emission from the atom at different pumping amplitudes Ω_{31}. With increasing Ω_{31}, the spontaneous emission peak broadens and then splits due to splitting of the ground state $|1\rangle$ by the Rabi frequency Ω_{31}. The emission in the more general case is calculated

analytically in [25] and well describes the split emission spectral line. Particularly, in the extreme case of $\Omega_{31} \gg (\gamma_{32}, \gamma_{21})$ each of the two split peaks is expressed as

$$S^{\pm}(\omega) \approx \frac{\rho_{22}\hbar\omega_{21}\Gamma_{21}}{2\pi} \frac{\gamma'/2}{\gamma'^2 + (\omega - \omega_{21} \pm \Omega_{31}/2)^2}, \quad (7)$$

where $\gamma' = (\gamma_{32} + \gamma_{21})/2$.

Eqs. (6) and (7) describe spectrum of the quantum noise in the system, determined by the spontaneous emission to the transmission line. The interaction with 1D open space (transmission line) characterized by Γ_{21} is enhanced in the field of an external resonant probe wave at the transition frequency ω_{21}, stimulating emission coherent with the external probe wave. We measure the amplitude and phase of transmission t as a function of detuning $\delta\omega_{21}$ under a relatively weak probe wave amplitude Ω_{21}, at different pumping amplitudes Ω_{31} [Fig. 3(a)]. The black curve, obtained at relatively weak pumping with $\Omega_{31}/2\pi = 3$ MHz, shows a Lorentzian dip with the linewidth of 40 MHz, determined mainly by the dephasing $2\gamma_{21}$. The transmission is strongly modified as Ω_{31} is increased. At $\Omega_{31}/2\pi = 23$ MHz, the dip is completely suppressed (blue curve). At stronger pumping, the amplification is observed: at $\Omega_{31}/2\pi = 40$ MHz (red curve) the transmission exceeds one by 5%, exhibiting a clear amplification peak, and at $\Omega_{31}/2\pi = 95$ MHz (green curve) the peak is split. Note that in the amplification condition, the phase on the lower panel of Fig. 3(a) is inverted. The intensity plots of Fig. 3(b) summarize the behavior of t versus pumping amplitude Ω_{31}.

The inset of Fig. 3(a) shows gain $|t|$ at the fixed pumping amplitude $\Omega_{31}/2\pi = 40$ MHz as a function of the probe amplitude Ω_{21}. In the linear amplification regime ($\Omega_{21}/2\pi < 20$ MHz), corresponding to the nearly constant $|t|$, the gain reaches maximum of about 1.09. Interestingly, the best agreement between the calculated (red) curve and the experimental data (black dots) is obtained when pure dephasing is neglected ($\gamma_{21} = \Gamma_{21}/2$). Indeed, t is insensitive to linear fluctuations of $\delta\omega_{21}$ in the "magic point" of $\Omega_{31} = 2\gamma_{32}$.

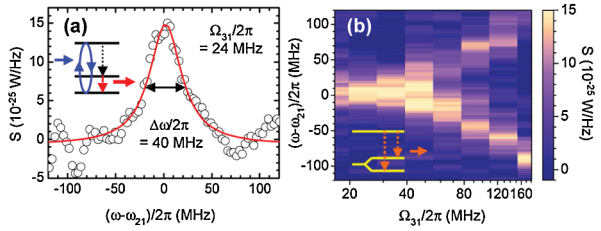

FIG. 2 (color). Spontaneous emission in the three-level atom. (a) Emission spectrum ($S = 2\pi S(\omega)$) measured in the vicinity of $\omega_{21}/2\pi = 10.96$ GHz [$\Phi = 3.5 \times 10^{-3}\Phi_0$; see Fig. 1(b)]. (b) Emission spectrum as a function of pumping amplitude Ω_{31}. At strong pumping, the emission peak is split by Ω_{31}, due to Rabi splitting of the level $|1\rangle$, as schematically depicted in the inset. The spontaneous emission spectrum gives the noise in the system.

Remarkably, the gain for the single atom amplifier is fundamentally limited by $\sqrt{2}$ (the corresponding power gain is 2), as each incident photon can stimulate not more than one emitted photon. Moreover, the photon multiplication factor is always less than 2, due to competing incoherent processes, for instance, relaxation caused by unavoidable quantum noise. The factor is reduced even more by less-than-100% population of the level $|2\rangle$. To calculate the maximal gain we consider the system in double resonance, without pure dephasing and with $\Gamma_{32} \gg \Gamma_{21}$. In such a case for driving amplitude of the order of threshold defined by Eq. (5), the populations can be simplified to $\rho_{11} = 1/(1 + \nu)$ and $\rho_{22} = \nu/(1 + \nu)$, where $\nu = \Omega_{31}^2/(\Gamma_{32}\Gamma_{21})$ is a square of normalized driving amplitude [25]. With this variable Eq. (4) becomes $t = 1 + (\nu - 1)/(\nu + 1)^2$, which takes maximum $t = 1 + 1/8$ at $\nu = 3$, that is $\Omega_{31}^2 = 3\Gamma_{21}\Gamma_{32}$ and the corresponding populations are $\rho_{22} = 3/4$ and $\rho_{11} = 1/4$.

We derive the parameters of our system from the experimental data. From the dip in the transmission in the absence of pumping [see Eq. (4) with $\Omega_{31} = 0$ and $\rho_{22} - \rho_{11} = -1$], $\Gamma_{21}/2\pi$ is found to be 11 MHz. In the case of negligible pure dephasing in γ_{31} ($=\Gamma_{32}/2$) and γ_{32} ($=\Gamma_{32}/2 + \Gamma_{21}/2$) [26], the experimental data are in a very good agreement with theory, when we take $\Gamma_{32}/2\pi = 35$ MHz [27]. Amplification occurs, when the pumping amplitude exceeds $\Omega_{31}/2\pi \approx 20$ MHz, found from Eq. (5) consistently with our experiment.

The six panels in Fig. 4, each measured at different Ω_{31}, show $|t|$ versus detuning from the resonances: $\delta\omega_{31}$ (x axis) and $\delta\omega_{21}$ (y axis). Amplification regions revealed as bright spots near the double resonance points, split at strong pumping ($\Omega_{31}/2\pi = 95$ MHz). The splitting is reminiscent of the typical anticrossing (shown by a black

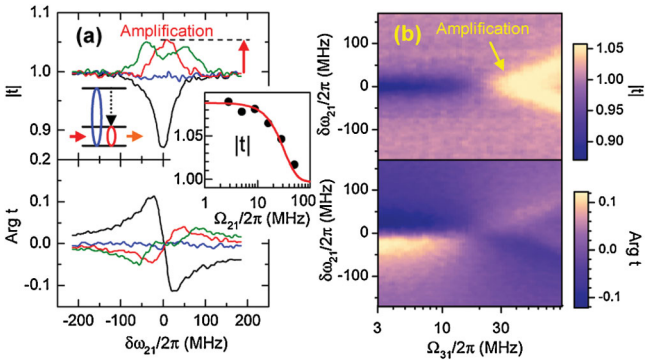

FIG. 3 (color). Amplification on the single three-level atom. (a) Amplitude and phase of the transmission coefficient t versus detuning from the resonant frequency $\omega_{21}/2\pi = 10.96$ GHz at a different pumping amplitudes Ω_{31}. The inset shows the amplification coefficient $|t|$ as a function of the probe amplitude Ω_{21} at $\delta\omega_{21} = 0$. (b) The intensity plot, summarizing the measurements shown in (a), demonstrates the transmission amplitude (upper panel) and phase (lower panel) as a function of the pumping amplitude Ω_{31}.

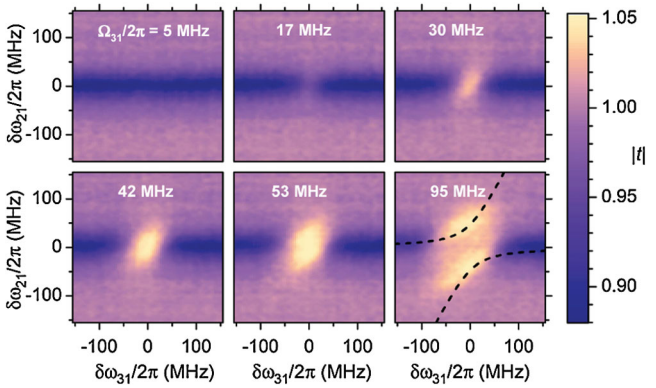

FIG. 4 (color). Amplification versus detuning of pumping and probe frequencies $\delta\omega_{32}$ and $\delta\omega_{21}$. The pumping amplitudes Ω_{31} are indicated on the panels. The black dashed line on the panel with the strongest pumping ($\Omega_{31}/2\pi = 95$ MHz) shows the expected anticrossing spectroscopy line.

dashed line); however, it reveals in the over-unity transmission $|t| > 1$ that is amplification.

The amplification by a single artificial atom provides an example of an elementary quantum amplifier. However, we suggest that it can be used as a building block for practical quantum amplifiers with the noise characteristics limited by quantum noise due to spontaneous emission to the open space. The demonstrated on-chip amplifier is tunable, and its bandwidth can be selected by changing coupling to the transmission line.

In a conclusion, we have demonstrated a fully controllable and tunable on-chip quantum amplifier with a single artificial atom in open 1D space. The work may open a direction of on-chip quantum electronics.

This work was supported by CREST-JST and MEXT kakenhi ''Quantum Cybernetics.''

*On leave from Lebedev Physical Institute, Moscow 119991, Russia.

†On leave from the Physical-Technical Institute, Tashkent 100012, Uzbekistan.

[1] M. O. Scully and M. S. Zubairy, *Quantum Optics* (Cambridge University Press, Cambridge, England, 1997).

[2] W. T. Silfvast, *Laser Fundamentals* (Cambridge University Press, Cambridge, England, 2004).

[3] J. Hwang, M. Pototschnig, R. Lettow, G. Zumofen, A. Renn, S. Götzinger, and V. Sandoghdar, Nature (London) **460**, 76 (2009).

[4] I. Gerhardt, G. Wrigge, P. Bushev, G. Zumofen, M. Agio, R. Pfab, and V. Sandoghdar, Phys. Rev. Lett. **98**, 033601 (2007).

[5] G. Wrigge, I. Gerhardt, J. Hwang, G. Zumofen, and V. Sandoghdar, Nature Phys. **4**, 60 (2008).

[6] M. K. Tey, C. Zilong, S. A. Aljunid, B. Chng, F. Huber, G. Maslennikov, and C. Kurtsiefer, Nature Phys. **4**, 924 (2008).

[7] A. N. Vamivakas, M. Atatüre, J. Dreiser, S. T. Yilmaz, A. Badolato, A. K. Swan, B. B. Goldberg, A. Imamoglu, and M. S. Ünlü, Nano Lett. **7**, 2892 (2007).

[8] A. Muller, E. B. Flagg, P. Bianucci, X. Y. Wang, D. G. Deppe, W. Ma, J. Zhang, G. J. Salamo, M. Xiao, and C. K. Shih, Phys. Rev. Lett. **99**, 187402 (2007).

[9] G. Zumofen, N. M. Mojarad, V. Sandoghdar, and M. Agio, Phys. Rev. Lett. **101**, 180404 (2008).

[10] J. M. Raimond, M. Brune, and S. Haroche, Rev. Mod. Phys. **73**, 565 (2001).

[11] C. J. Hood, T. W. Lynn, A. C. Doherty, A. S. Parkins, and H. J. Kimble, Science **287**, 1447 (2000).

[12] D. Englund, A. Faraon, I. Fushman, N. Stoltz, P. Petroff, and J. Vučković, Nature (London) **450**, 857 (2007).

[13] A. Wallraff, D. I. Schuster, A. Blais, L. Frunzio, R.-S. Huang, J. Majer, S. Kumar, S. M. Girvin, and R. J. Schoelkopf, Nature (London) **431**, 162 (2004).

[14] D. I. Schuster *et al.*, Nature (London) **445**, 515 (2007).

[15] M. Hofheinz *et al.*, Nature (London) **459**, 546 (2009).

[16] D. Meschede, H. Walther, and G. Müller, Phys. Rev. Lett. **54**, 551 (1985).

[17] J. McKeever, A. Boca, A. D. Boozer, J. R. Buck, and H. J. Kimble, Nature (London) **425**, 268 (2003).

[18] O. Astafiev, K. Inomata, A. O. Niskanen, T. Yamamoto, Yu. A. Pashkin, Y. Nakamura, and J. S. Tsai, Nature (London) **449**, 588 (2007).

[19] M. Nomura, N. Kumagai, S. Iwamoto, Y. Ota, and Y. Arakawa, Nature Phys. **6**, 279 (2010).

[20] J.-T. Shen and S. Fan, Phys. Rev. Lett. **95**, 213001 (2005).

[21] D. E. Chang, A. S. Sørensen, E. A. Demler, and M. D. Lukin, Nature Phys. **3**, 807 (2007).

[22] O. Astafiev, A. M. Zagoskin, A. A. Abdumalikov, Jr., Yu. A. Pashkin, T. Yamamoto, K. Inomata, Y. Nakamura, and J. S. Tsai, Science **327**, 840 (2010).

[23] J. E. Mooij, T. P. Orlando, L. Levitov, L. Tian, C. H. van der Wal, and S. Lloyd, Science **285**, 1036 (1999).

[24] A. A. Abdumalikov, Jr., O. Astafiev, Y. Nakamura, Yu. A. Pashkin, and J.-S. Tsai, Phys. Rev. B **78**, 180502(R) (2008).

[25] See supplementary material at http://link.aps.org/supplemental/10.1103/PhysRevLett.104.183603 for the detailed theoretical analysis and the measurement scheme.

[26] We can neglect pure dephasing in γ_{32} and γ_{31}, because, first, it is expected to be much weaker than γ_{21}, due to less steep energy bands, and, second, relaxation Γ_{32} is strong ($\Gamma_{32} \gg \gamma_{21}$). Note also that $\Gamma_{31} \ll (\Gamma_{32}, \Gamma_{21})$.

[27] The experimentally derived Γ_{32} is about twice higher than the expected one for 50 Ω impedance. We suppose that this is a signature of frequency dependent impedance above 13 GHz, which we could not control in our experiments.